Viability to Predict Driver Intentions in Unmarked Roundabouts using vehicle and contextual information

R. Vazquez
Universidad Tecnológica Nacional
Facultad Regional Resistencia
Resistencia, Argentina
e-mail: rayvazquez2005@ca.frre.utn.edu.ar

F. R. Masson
Universidad Nacional del Sur - CONICET
Instituto de Investigaciones en Ingeniería Eléctrica
Depto. de Ingeniería Eléctrica y de Computadoras
Bahía Blanca, Argentina
email: fmasson@uns.edu.ar

Abstract

As the demand for advanced driver assistance systems (ADAS) and autonomous driving technologies increases, accurate predictions of driver intentions in complex scenarios, such as unmarked roundabouts, become crucial. This study presents a predictive model based on Long Short-Term Memory (LSTM) neural networks that integrates kinematic motion data, vehicle positioning, and road texture analysis to anticipate whether a driver intends to turn right, turn left, or continue straight when approaching a roundabout. The model was validated using real-world data collected at unsignalized roundabouts, demonstrating effective and accurate intention prediction in practical applications. By processing data within a 20-second moving window and updating predictions every second, the approach enables continuous real-time assessment of driver intentions. These results highlight the potential of the proposed model to enhance the functionality of ADAS, particularly in environments without clear road signs. Future work will focus on expanding the dataset, refining the analysis of contextual features, and adapting the model to a wider range of traffic scenarios to further improve its robustness and generalization.

Keywords – driver intention prediction, roundabout navigation, LSTM neural network

1. Introduction

Driving a vehicle is a specialized task that requires a deep understanding of the specific contexts in which drivers operate. This understanding is crucial for safe movement in high-traffic areas. Although navigation may seem trivial for an experienced human driver, discerning the intentions of other drivers presents a significant challenge. This challenge is particularly relevant in advanced driver assistance systems (ADAS).

Intersections and roundabouts present specific problems due to the coordination required among multiple vehicles. Models supporting the development of motion planning strategies are essential to facilitate appropriate decision making in these scenarios. The complexity emerges from uncertainties about the intentions and destinations of surrounding vehicles, aggravated by visual obstructions and vehicle movements at intersections.

Recent studies have shown that the use of turn signals is influenced by various demographic and contextual factors, including the presence of secondary tasks while driving and the type of intersection

(urban or rural). In particular, [1] identified that drivers use turn signals less frequently when distracted by secondary tasks, and that signaling rates are higher in urban areas and at intersections without dedicated turning lanes. These observations support the importance of considering driver behavior and contextual factors when developing predictive models for maneuver intentions in unmarked intersections.

To address these complexities, several approaches have been explored. Initially, strategies were developed to enhance intersection safety by coordinating traffic through vehicle-to-vehicle and vehicle-to-infrastructure communications [2]. Subsequent research efforts have focused on creating interaction models that integrate environmental signals to interpret them and detect objects [3].Analyzing vehicle trajectories with anticipation of potential destinations has been explored using long-short-term memory (LSTM) neural networks [4].Further investigations have utilized artificial vision systems [5,6] and collected in-cabin data such as steering wheel hand position, pedal foot placement, and driver's gaze and head movement, including turn signal status [7].

At present, Deep Learning techniques, which involve a set of algorithms for extracting patterns from large datasets, are employed to enhance these models. Specifically, these techniques leverage neural network architectures capable of learning hierarchical representations of data, improving the model's ability to predict driver intentions and actions. By processing vast amounts of data, Deep Learning models can identify subtle patterns and correlations that are often missed by traditional methods. This approach has not only improved prediction accuracy, but has also increased the robustness and generalizability of the models in different driving scenarios [8].

In addition to traditional methods for traffic estimation and driver behavior analysis, machine learning-based models have been explored for their advantages in dynamic environments. For example, [9] compared the classical HCM method with a machine learning-based vision system for measuring delays at intersections, finding that the modern approach better captures real-time fluctuations. These results support the notion that deep learning models, like the one proposed in this study, can overcome the limitations of conventional methods and offer more accurate predictions in complex scenarios such as unmarked roundabouts.

This study aims to develop a predictive model for the intentions of drivers in unmarked roundabouts that integrates dynamic vehicle information, interactions with infrastructure, and texture analysis from images within the driver's visual field. This document includes five sections. Section II details the methodology used to develop the predictive model. Section III presents the model, integrating dynamic vehicle information and texture analysis. Section IV presents the results obtained from dynamic vehicle data and sensor fusion using an LSTM network. Section V discusses the conclusions and explores potential future research directions.

2. Description of Components for Predicting Driver Intentions in Unsignalized Roundabouts

In recent years, research on driver behavior has focused primarily on well-structured environments with clearly defined lanes and traffic signals [10][11]. However, less attention has been paid to more challenging scenarios, such as unmarked roads, where the lack of clear infrastructural guidance can lead to a wide set of driving behaviors. This variability introduces significant complexity when analyzing the intentions of drivers at intersections and roundabouts, where the path is inherently non-linear and traditional physical models often fail [12]. Recent studies, such as [13], have highlighted that the

inclusion of specific infrastructural elements—like free-flow right-turn bypass lanes at single-lane roundabouts—can notably influence overall delay and traffic performance. These findings underscore the importance of incorporating such design factors in understanding and predicting driver intentions at unsignalized roundabouts.

Recognized worldwide for their efficiency in managing traffic flow in low- to medium-traffic zones, roundabouts are a common type of unsignalized intersection. These structures range from tangential to radial designs, often improving visibility and safety. Despite their benefits, navigating roundabouts can be unpredictable due to the uncertain intentions of other drivers and the absence of traffic signals.

This study introduces a method to identify the intentions of drivers, whether to turn right (TR), turn left (TL), or go straight (GS) – using a 'time window' technique [14]. The approach analyzes the kinematic and dynamic variables of the vehicle over a defined time interval as it approaches the roundabout. Using this specific time window, the method captures indicators of driver behavior, which are then used to predict the intended maneuver. This approach is designed to operate in environments with multiple potential driver actions and unpredictable surrounding traffic. Figure 1 illustrates the configuration of the time window, initiated 40 meters before the start of the roundabout.

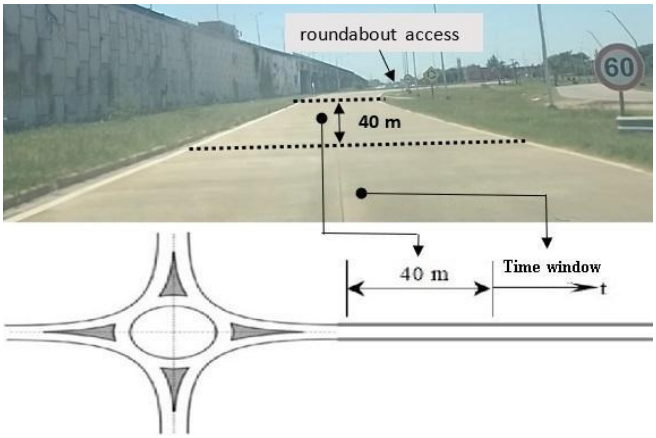

Fig. 1. Simplified diagram of data collection.

Figure 2 shows the trajectory of a vehicle the considered intentions. Figure 2.a visualizes the trajectory of a vehicle with GS intention, Figure 2.b with TR intention, and Figure 2.c with TL intention. Trajectories were captured using GPS receiver mounted on the hood of the vehicle and recorded at 1-second intervals.

The MPU6050 gyroscope, coupled with the GPS, ensures precise measurement of the vehicle's movement dynamics. The data logger records additional relevant variables, such as longitude, latitude, and distance traveled. In addition, a vehicle camera mounted on the windshield captures high-resolution video of the drives, providing a visual record of the trajectories. Figure 3 shows the location of the data logger in the car.

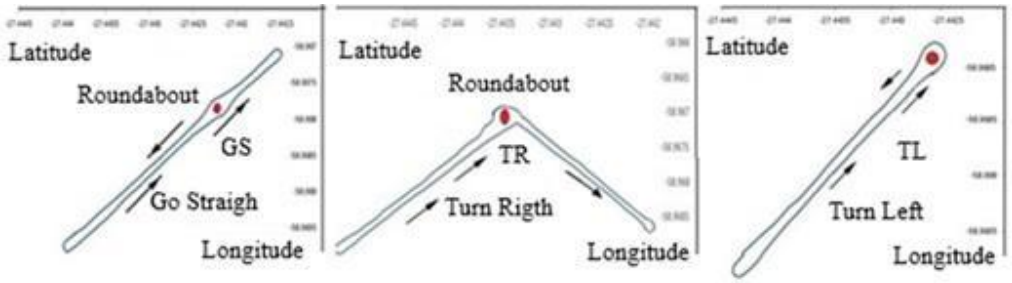

(a) (b) (c)

Fig. 2. Vehicle trajectory intentions considered: (a) go straight (GS), (b) turn right (TR), (c) turn left (TL)

Fig. 3. Vehicle used in the study.

To collect data, a 150-meter time window was established starting 40 meters before the roundabout to capture the vehicle's position, velocity, and acceleration along both the X and Y axes. This window enables a continuous data stream that reflects the vehicle's approach and navigation through the roundabout. Key measurements, including GPS location, lateral and longitudinal velocities, and acceleration, are recorded to create a detailed sequence of driver behaviors. The data obtained during this interval feed into the predictive model to enhance its accuracy in anticipating the driver's maneuver intention, whether turning left, right, or continuing forward.

2.1 *Methodology for Vehicle Trajectory Analysis Using Fixed Reference Points and Kinematic Equations in Roundabouts*

In our methodology, we use two fixed reference points, labeled P_1 and P_2. The first reference point, P_1, is in the center of the roundabout. The second point, P_2, is diagonally positioned relative to a fixed axis parallel to the avenue and passing through P_1. This placement allows for the measurement of angles

formed by segments A and B, as shown in Figure 4. The distance between P_1 and P_2 is defined as segment C. This segment corresponds to the shortest distance from the roundabout center to the adjacent street corner, which in practice is given by the tip of the block edge. In our experimental setup, this criterion resulted in a fixed value of 16.2 meters. The position of P_2 helps to track vehicle trajectories and direction changes, providing data for analysis. Furthermore, a mobile point, P, moves with the vehicle, represented by its coordinates x_i and y_i.

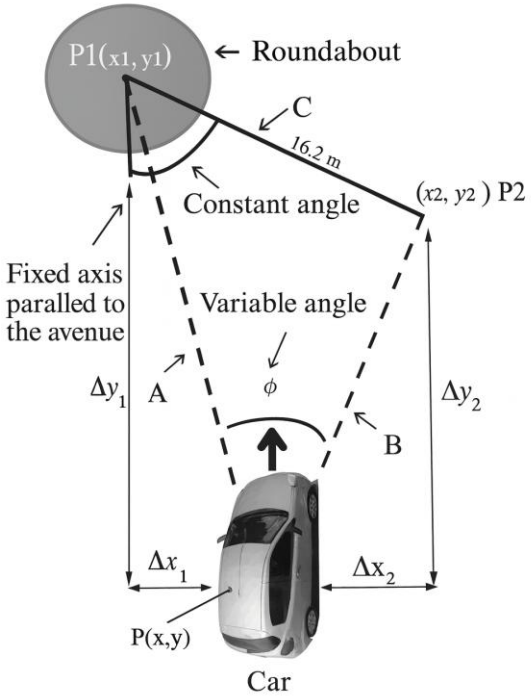

Fig. 4. Vehicle positioning for roundabouts, incorporating fixed reference points and kinematic modeling.

The distances A_i and B_i from the vehicle to P_1 and P_2 respectively are calculated using equations (1) and (2):

$$A_i = \sqrt{(x_1 - x_i)^2 + (y_1 - y_i)^2} \quad (1)$$

$$B_i = \sqrt{(x_2 - x_i)^2 + (y_2 - y_i)^2} \quad (2)$$

Subsequent calculations for the differences are as follows:

$$\Delta y_1 = y_1 - y_i \quad (3)$$

$$\Delta y_2 = y_2 - y_i \quad (4)$$

$$\Delta x_1 = x_1 - x_i \quad (5)$$

$$\Delta x_2 = x_2 - x_i \quad (6)$$

Using equations (1) and (2), ϕ_i is then derived as:

$$\phi_i = arcos\left(\frac{{A_i}^2 + B_i^2 - C^2}{2.A_i.B_i}\right) \quad (7)$$

Where C is the shortest distance between the roundabout center and the adjacent street corner, which in our experimental setup corresponds to 16.2 m. For example, when a driver intends to make a right turn, segment B shows a more pronounced rate of decrease compared to segment A. As the vehicle approaches the roundabout, the values of ϕ increase, reflecting the change in position relative to the center of the roundabout. This principle applies similarly to Δx_1 and Δx_2, which represent the relative horizontal distances from the reference points. The computed values for ϕ, Δx_1, and Δx_2 are then classified according to the intended maneuver of the driver (for example, turning right, left, or straight). These categories are structured into a dataset, segmented into nine distinct columns. These columns, which represent various positional and kinematic data points, serve as input features for the neural network, helping it learn and predict the driver's intentions. In the context of the network, each column represents a unique input feature utilized to train and test the model.

2.2. Predict Vehicle Trajectories

To evaluate the effectiveness of combining vehicle trajectory and kinematic data, a dataset was collected in an unmarked roundabout by a single driver on different days and under varying traffic conditions. An LSTM network was used as the inference model. These networks are suitable for time series analysis [15] and for predicting vehicle trajectories in roundabouts [16]. The model used in this study is shown in Figure 5. The "Dataset" block contains the training and testing data, and the "Data Output" block contains the outputs. The output layer has three classes: TR (Turn Right), TL (Turn Left), and GS (Go Straight).

The network was trained with the Adam optimizer, binary cross-entropy loss, and accuracy as the evaluation metric. The training used a batch size of 32 for 20 epochs. Data came from equations (1) to (7), with segment C equal to 16.2 meters, producing 300 instances. Each time step, defined as 20 seconds, included GPS data sampled every second and gyroscope data with x and y accelerations also sampled every second. The model applies a 20-second moving window: each second, the oldest point is removed, and a new one is added. This allows real-time predictions of driver intent, updated every second, as the vehicle approaches the roundabout. A "time step" refers to one interval of data showing the vehicle's position and kinematic state at that instant.

To address the limitation of only 300 real cases, the dataset was expanded to 3000 samples through data augmentation (rotation, stretching, translation), following methods used in related studies [17].

This increased the dataset size while keeping kinematic consistency and adding variability for robust training.

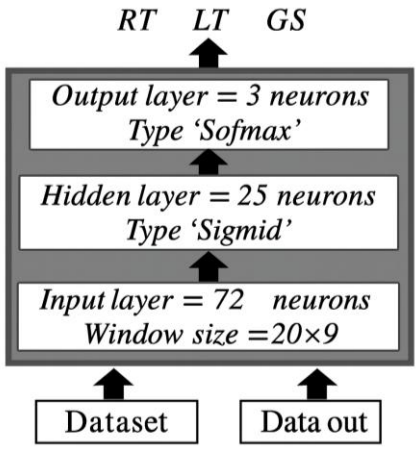

Fig. 5. LSTM network used in the experiment.

The dataset is divided equally with 1500 examples allocated for training and another 1500 for testing. The properties of the experimental data are detailed in Table 1.

Tab 1. Characteristics of experimental data.

Features	Number
Dataset	3000
Training	1500
Test	1500
Time step (sec)	20

This model provides a 40-meter prediction window to anticipate driver intentions to go straight, turn right, or turn left when approaching the roundabout. As shown in Figure 6 (a), the model reaches stability after approximately 15–18 iterations, with the training accuracy stabilizing around 0.62 and the test accuracy around 0.58. At the same time, the loss metrics converge to values close to 0.50 for training and 0.55 for testing, as illustrated in Figure 6 (b).

To train the LSTM network, we use the TensorFlow tool [18]. The Receiver Operating Characteristic (ROC) curve [19], depicted in Figure 6 (b), serves as a graphical representation to illustrate the trade-off between sensitivity and specificity in a classifier system as the discrimination

threshold is varied. In this scenario, Class 0 corresponds to "Turn Right" (TR), Class 1 to "Go Straight" (GS), and Class 2 to "Turn Left" (TL).

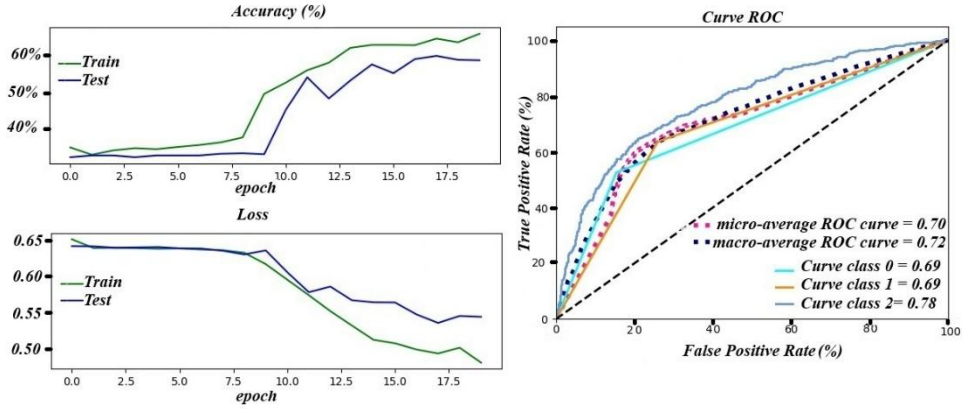

(a) (b)

Fig. 6. (a) Training response from the LSTM network; (b) ROC curve for the three maneuver cases.

As can be seen, there is potential to improve these results, and one possibility is to incorporate contextual information through image processing. The following section will focus on the specific case of unmarked roundabouts, highlighting the importance of integrating multiple parameters and perception techniques to improve lane detection in ADAS systems, including the relative positions of nearby vehicles.

3. Image Processing for Lane Detection Systems

The traffic context acts as a primary factor that influences driver intentions, and understanding it allows an accurate prediction of driver behavior. The capability of detecting and monitoring nearby vehicles, either ahead or alongside them, enables effective real-time analysis of lane occupancy and potential lane changes. The design of the lane markings, whether continuous or dashed, indicates the legality of lane changes in various directions. Thus, both the traffic context and the perception of the road play an important role in determining driver intentions.

In our case, we are interested in roundabouts without demarcation lines. Through image processing techniques, a vehicle lane detection system is developed that analyzes histograms and textures to improve accuracy. Figures 7, show the views captured by a driver navigating an unmarked road within the defined road window. The first figure represents the left side and the right side, the second the center. We proposed a camera positioned in the top center of the car to record these scenes.

(a) (b)

Fig. 7. Vehicle traveling in the left lane (a) ,right lane (b) and center lane (c).

In this study, we used five rectangular regions within the driver's field of view (yellow rectangles) to facilitate the analysis of textures and grayscale values on unmarked roads. The YOLOv3 [20] object detection model was used to verify the absence of vehicles within these regions, ensuring that the visual data captured is exclusive to the road surface.

The locations of the five rectangles are strategically placed. Three to cover the center of the unmarked road, while the remaining two were placed on the left and right sides. In cases where the YOLOv3 model detects vehicles within the texture analysis regions, the corresponding images are discarded to avoid distortions in the texture data. This approach ensures that input data remain free from obstructions and maintains the accuracy of the model. Future work may explore adjusting the position or size of the analysis regions to reduce the occurrence of these obstructions, allowing greater continuity in data collection. This distribution allows the model to accurately capture the relevant grayscale and texture information from different areas of the road, contributing to the effective extraction of features from the rectangular sections. The central rectangles ensure complete coverage of the main path, where most decisions are made. The lateral rectangles, covering the left and right edges, provide additional data from peripheral areas that may influence lane changes or other maneuvers.

The Local Binary Pattern (LBP) descriptor, used to automatically classify and identify textures [21], computes a descriptor for each image point, encoding the relationship of each pixel to its neighbors as a numerical value. Uniform patterns of LBP are specifically chosen for their ability to reduce feature vector dimensionality and enhance classifier performance, also providing rotation invariance. A uniform LBP pattern, which contains at most two transitions between binary states, is defined as LBPU (e.g., 000100 is LBPU with two transitions, whereas 010101001 with seven transitions is not). When compiling the LBP histogram, each uniform pattern receives a unique value, while all non-uniform patterns are grouped under a single value, thus reducing the feature vector dimensionality. The skimage library facilitates the computation of LBPU descriptors. The LBPU histograms for the left, right, and middle lanes are illustrated in Figures 8 (a), 9 (b), and (c), respectively.

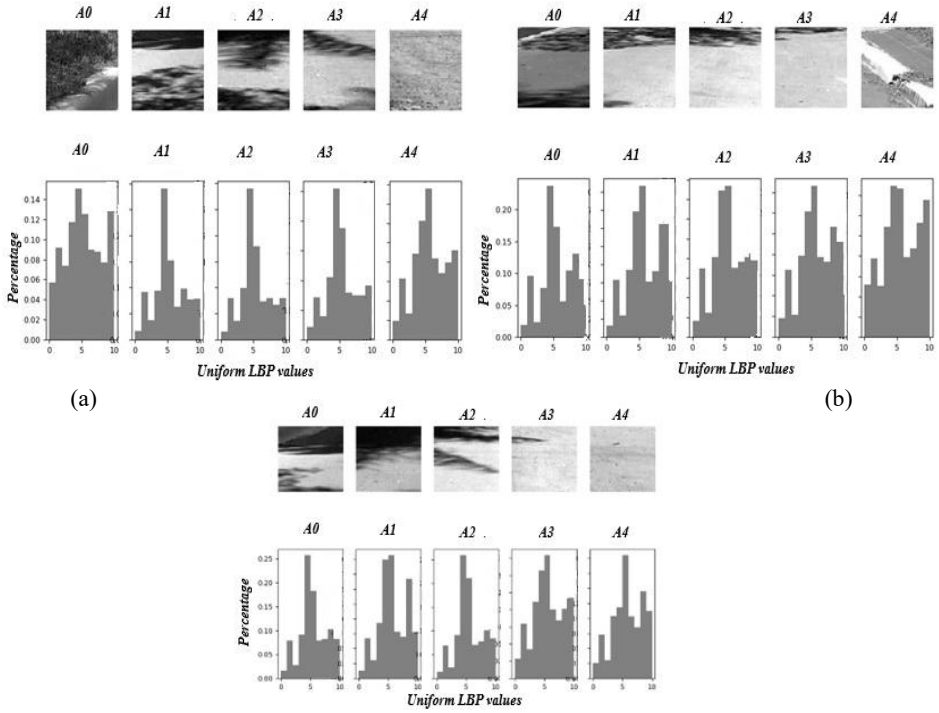

(a) (b)

(c)

Fig. 8. (a) LBPU histogram for the left lane, (b) LBPU histogram for the right lane, (c)LBPU histogram for the middle lane.

The Kullback-Leibler divergence is utilized as a mathematical operator to compare histogram distributions. It calculates the divergence between the central area A2 and adjacent areas A0, A1, A3, and A4. The resulting values are summarized in Tables 2, 3, and 4.

Tab 2. Divergence metrics for the left lane.

Row	Area	Texture (LBP)
1	A0 and A2	0.11486
2	A1 and A2	0.00636
3	A3 and A2	0.00593
4	A4 and A2	0.06223

Tab 3. Divergence metrics for the middle lane.

Row	Area	Texture (LBP)
1	A0 and A2	0.00370
2	A1 and A2	0.02713
3	A3 and A2	0.05223
4	A4 and A2	0.07251

Tab 4. Divergence metrics for the right lane.

Row	Area	Texture (LBP)
1	A0 and A2	0.02417
2	A1 and A2	0.01757
3	A3 and A2	0.01102
4	A4 and A2	0.04116

Essentially, lower divergence values suggest greater similarity between textures, indicative of similar driving conditions or vehicle behaviors. Data analysis reveals higher divergence values in specific rows, suggesting differing vehicle positions within lanes. For example, a higher divergence in the first row of Table 2 suggests the presence of a vehicle in the left lane, while lower values in the fourth row of Table 4 imply the proximity of the vehicle to the right lane. Although the divergence values in Table 3 show variation, they generally remain low, highlighting the nature of these measurements. The information presented in this section will be integrated with Section II as detailed below.

4. Integrated Methodology for Driver Intention Prediction

The primary objective of this study is to develop a comprehensive model to predict driver intentions by integrating dynamic vehicle data, interactions with infrastructure, and contextual insights derived from road images. This model employs an integrated approach that combines various data streams to improve the accuracy and reliability of the prediction. Figure 9 summarizes the proposed model. The dynamic data collected from the vehicle, along with two categories of sensor-derived data, are processed and integrated within this model.

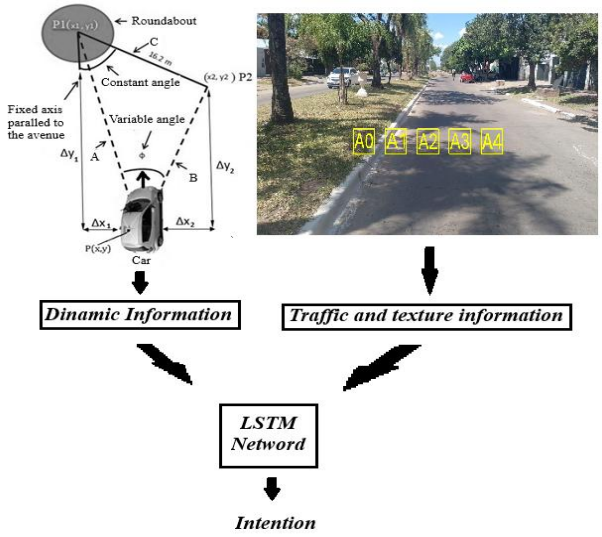

Fig. 9. Proposed Intention Model. Vehicle information (position, accelerations, and angular velocities), infrastructure interaction, and contextual road and traffic information are input into an LSTM network.

When YOLOv3 detects that there are no vehicles, image processing is performed to analyze the textures and histogram, as described in the previous section. This uses visual information obtained through image processing. Techniques such as object detection with YOLOv3 and texture analysis (LBP) are used to extract key parameters, such as the comparison of values illustrated in Tables 2 to 4. This information is then used to estimate the position of the vehicle on the road. Each possible position is assigned a predefined number: for example, 1 for the left lane, 2 for the center lane, and 3 for the right lane. The classification of these positions is determined on the basis of a set threshold instead of introducing texture divergence directly into the neural network. This choice reduces computational complexity and focuses the model on predicting the intended maneuver based on predefined positional categories. Future work may explore the direct integration of divergence values as inputs to the network to allow the model to learn lane positions without predefined thresholds.

The result of this analysis is added as a new column to the dataset, representing the vehicle's position on the road. This column is incorporated as the tenth column in the dataset, making the new training set 20x(7+2+1). This complete set forms the LSTM block shown in Figure 11. This procedure is applied to three videos, each representing a different position of the lane: left, center, and right.

A texture threshold and grayscale histogram scale are defined for the left, center, and right lanes. The results are stored in a file, following these steps, for example:

- *Start the central lane video.*
- *YOLOv3 does not detect vehicles in the representative window of the driver's field of view.*
- *The texture values are obtained.*

From these data, the driver's intention is determined. This process is repeated with intentions of turning left or right, depending on the video used. The obtained values are added as a new column to the previously calculated training data. The process is then repeated, and a new model is generated that incorporates the texture.

5. Experimental Results and Comparative Analysis

The training of the LSTM network with the 9-feature dataset showed that the model reached stability after approximately 180 iterations, with a final accuracy of 0.91 and a loss of 0.35. Figure 10 presents these results: (a) the training response of the LSTM network, and (b) the ROC curve for the three maneuver intention classes (Turn Right, Go Straight, Turn Left).

These results suggest that the inclusion of additional variables in the training and validation phases, compared with the setup described in Section II, is associated with observable improvements in predictive performance across the three intention categories.

.

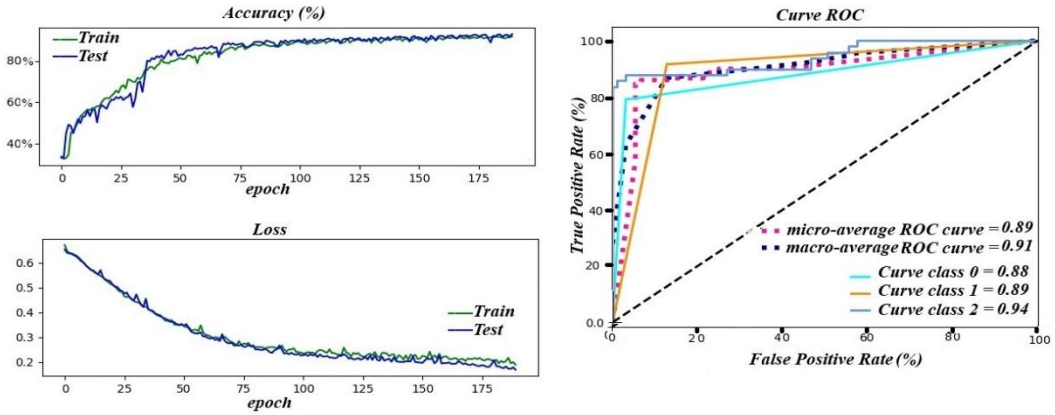

(a) (b)

Fig. 10. (a) Training response from the LSTM network. (b) ROC curve using data fusion.

The classification capabilities of the model are organized into three distinct classes: Class 0 for TR (turn right), Class 1 for GS (go straight), and Class 2 for TL (turn left). This structured approach improves the model's ability to accurately predict driver intentions, as demonstrated in Figure 10 (b).

Additionally, a comparative evaluation was carried out including both classical and deep learning predictors (Logistic Regression, Decision Tree, CNN, RNN, Hybrid CNN-RNN, and LSTM) under 9- and 10-feature configurations. Table 4 (Comparative Metrics Table) consolidates the results, while Figures 11 and 12 (Accuracy and F1 Score Comparison) provide a visual representation of the differences.

With 9 features, the models demonstrated limited predictive capacity. Logistic Regression and Decision Tree achieved accuracies of 0.46 and 0.37, respectively. CNN, RNN, and the hybrid CNN-RNN

reported values between 0.44 and 0.45, while the LSTM obtained a slightly higher accuracy of 0.57. However, across all models, macro-averaged precision, recall, and F1 scores remained low, and AUC values did not exceed 0.77.

Tab 5. Comparative Metrics

Model	Features	Accuracy	Precision (Macro)	Recall (Macro)	F1 Score (Macro)	AUC (OVR)
Logistic Regression	9	0.4627	0.4627	0.4627	0.4623	0.6376
Decision Tree	9	0.3713	0.3713	0.3713	0.3711	0.5285
Logistic Regression	10	0.8227	0.8228	0.8227	0.8219	0.9367
Decision Tree	10	0.9673	0.9673	0.9673	0.9673	0.9755
CNN	9	0.4483	0.4563	0.4483	0.4454	0.6399
RNN	9	0.4533	0.4543	0.4533	0.4528	0.6402
Hybrid CNN-RNN	9	0.4517	0.4534	0.4517	0.4509	0.6354
CNN	10	0.9467	0.9506	0.9467	0.9464	0.9923
RNN	10	0.9633	0.9638	0.9633	0.9633	0.9938
Hybrid CNN-RNN	10	0.9600	0.9606	0.9600	0.9600	0.9944
LSTM	9	0.5707	0.6140	0.5740	0.5627	0.7682
LSTM	10	0.9380	0.9390	0.9370	0.9373	0.9899

In contrast, with 10 features, all models showed a substantial improvement. Logistic Regression reached 0.82 accuracy and an AUC of 0.93, while the Decision Tree achieved nearly perfect performance with 0.97 accuracy and 0.97 AUC. CNN reached 0.94 accuracy, RNN 0.96, and the hybrid CNN-RNN 0.96, all with AUC values above 0.99. The LSTM also achieved 0.93 accuracy with a 0.99 AUC, confirming its ability to generalize effectively in sequential data

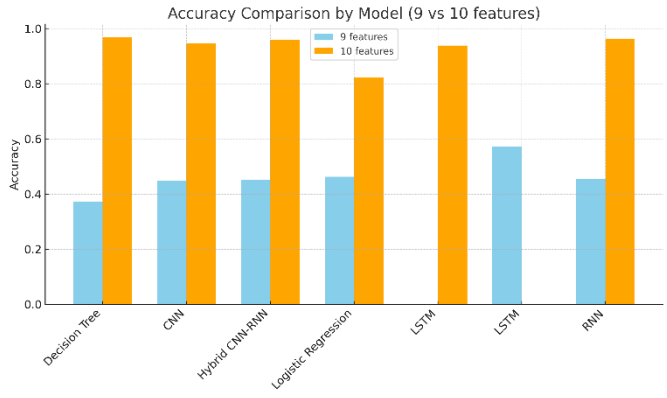

Fig. 11. Accuracy comparison of classical and deep learning models using 9 and 10 features.

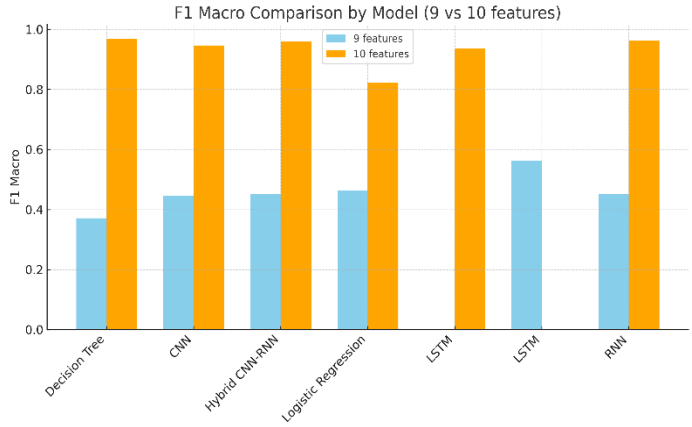

Fig. 12. F1 Score comparison of classical and deep learning models using 9 and 10 features.

The results indicate that the performance of all models improves markedly when moving from 9 to 10 features. With 9 features, both classical models (Logistic Regression and Decision Tree) and neural

networks (CNN, RNN, LSTM) achieve relatively low accuracies, ranging from 0.37 to 0.57. When using 10 features, however, the metrics increase substantially: Logistic Regression reaches 0.82, the Decision Tree approaches 0.97, and deep networks (CNN, RNN, Hybrid CNN-RNN, and LSTM) achieve between 0.93 and 0.96, with AUC values consistently above 0.99.

Overall, these results suggest that the tenth feature—derived from contextual road texture analysis—provides additional information that contributes to maneuver intention classification. This contribution is reflected in the improvements observed across both classical algorithms and neural network architectures, indicating progress in the reliable identification of driver intentions in unmarked roundabouts.

While the inclusion of the tenth feature improves the performance of all predictors, in some cases surpassing the LSTM, this advantage depends on the full availability of the feature set. In real-world applications, however, failures in object detection (e.g., when YOLOv3 does not identify obstacles in the forward view) may lead the system to revert to a reduced configuration with nine features. Under these conditions, the LSTM demonstrates superior or at least acceptable performance compared to other models, emphasizing its robustness in degraded scenarios. This observation aligns with previous studies, where LSTM networks are often employed in driver intention prediction due to their capacity to capture temporal dependencies, withstand noise, and maintain predictive accuracy even when information is incomplete or uncertain.

Although other predictors surpass the LSTM when the complete 10-feature set is available, their performance degrades more severely under reduced input conditions. In practical deployments, failures in object detection (e.g., YOLOv3 not identifying vehicles within the analysis window) may force the system to revert to a 9-feature configuration. In these cases, the LSTM demonstrates greater resilience, maintaining acceptable performance where other models deteriorate significantly. This robustness is consistent with prior studies, which emphasize the suitability of LSTM architectures for intention prediction tasks in noisy and uncertain environments, given their ability to capture temporal dependencies and mitigate the effects of missing or corrupted data.

Detailed information on the model configuration and its performance metrics is cataloged and can be accessed at [22]. This documentation is organized in accordance with the various sections covered in this research, facilitating easy navigation and understanding of the model's framework and capabilities.

6.Conclusion

This study introduced an LSTM-based predictive model for anticipating driver intentions in unsignalized roundabouts, integrating kinematic variables, vehicle positioning, and contextual road texture features. Comparative evaluation demonstrated that while all models benefit from feature expansion, the LSTM offers greater resilience under degraded conditions, such as reduced feature availability caused by detection failures. This robustness highlights its suitability for deployment in real-world ADAS applications where noise, occlusion, and incomplete information are frequent challenges.

The current validation, although limited to a single driver and location, provides a solid foundation for future research. Expanding data collection to include diverse drivers, roundabouts, and environmental conditions will improve generalizability. Future work should also investigate alternative

time-window configurations, adaptive thresholds for texture divergence, and methods to retain data when vehicles occlude texture regions, rather than discarding frames. Direct integration of texture divergence values into the LSTM model may further enhance predictive flexibility and robustness.

Overall, the findings suggest that LSTM-based architectures, due to their ability to capture temporal dependencies and withstand uncertainty, represent a promising direction for advancing intention prediction in complex and unsignalized traffic environments.

References

1. Ismaeel, R., M. Ajmal, and U. Gazder. ”What demographic and contextual factors predict drivers’ turn signal usage at junctions?.” *Advances in Transportation Studies* 65 (2025).
2. Debada, E. G., and D. Gillet. ”Virtual vehicle-based cooperative maneuver planning for connected automated vehicles at single-lane roundabouts.” *IEEE Intelligent Transportation Systems Magazine* 10, no. 4 (2018): 35–46.
3. Zyner, A., S. Worrall, and E. Nebot. ”A recurrent neural network solution for predicting driver intention at unsignalized intersections.” *IEEE Robotics and Automation Letters* 3, no. 3 (2018): 1759–1764.
4. Ohn-Bar, E., A. Tawari, S. Martin, and M. M. Trivedi. ”On surveillance for safety critical events: In-vehicle video networks for predictive driver assistance systems.” *Computer Vision and Image Understanding* 134 (2015): 130–140.
5. Alahi, A., K. Goel, V. Ramanathan, A. Robicquet, L. Fei-Fei, and S. Savarese. ”Social LSTM: Human trajectory prediction in crowded spaces.” In *Proceedings of the IEEE Conference on Computer Vision and Pattern Recognition*, 961–971. (2016).
6. Vicente, F., Z. Huang, X. Xiong, F. De la Torre, W. Zhang, and D. Levi. ”Driver gaze tracking and eyes off the road detection system.” *IEEE Transactions on Intelligent Transportation Systems* 16, no. 4 (2015): 2014–2027.
7. Luu, V. T., V. C. Huynh, V. H. Tran, T. H. Nguyen, and T. N. H. Phu. ”Traditional method meets deep learning in an adaptive lane and obstacle detection system.” In *2020 5th International Conference on Green Technology and Sustainable Development (GTSD)*, 148–152. IEEE. (November 2020).
8. Matzka, S., A. M. Wallace, and Y. R. Petillot. ”Efficient resource allocation for attentive automotive vision systems.” *IEEE Transactions on Intelligent Transportation Systems* 13, no. 2 (2012): 859–872.
9. Cho, N., A. Hainen, E. Tedla, and S. Burdette. ”A comparison of machine learning-based method vs. the Highway Capacity Manual method of intersection delay.” *Advances in Transportation Studies* 65 (2025).
10. Streubel, T., and K. H. Hoffmann. ”Prediction of driver intended path at intersections.” In *2014 IEEE Intelligent Vehicles Symposium Proceedings*, 134–139. IEEE. (June 2014).
11. Zyner, A., S. Worrall, and E. M. Nebot. ”ACFR five roundabouts dataset: Naturalistic driving at unsignalized intersections.” *IEEE Intelligent Transportation Systems Magazine* 11, no. 4 (2019): 8–18.

12. Ortega, P., C. Oliva, J. Ferland, and M. Cepeda. ”Multiple ant colony system for a VRP with time windows and scheduled loading.” *Ingeniare. Revista chilena de ingeniería* 17, no. 3 (2009): 393–403.
13. Mavromatis, S., A. Dimitriadou, V. Matragos, and F. Fotos. ”Assessment of free flow bypass lanes at single-lane roundabouts.” *Advances in Transportation Studies* 63 (2024).
14. Li, Y., L. Xin, D. Yu, P. Dai, J. Wang, and S. E. Li. ”Pedestrian trajectory prediction with learning-based approaches: A comparative study.” In *2019 IEEE Intelligent Vehicles Symposium (IV)*, 919–926. IEEE. (June 2019).
15. Zyner, A., S. Worrall, and E. Nebot. ”Naturalistic driver intention and path prediction using recurrent neural networks.” *IEEE Transactions on Intelligent Transportation Systems* 21, no. 4 (2019): 1584–1594.
16. Gulli, A., and S. Pal. *Deep Learning with Keras: Implement Neural Networks with Keras on Theano and TensorFlow.* Packt, 2017.
17. Wu, J., Z. Xu, Y. Monno, and M. Okutomi. ”Trajectory data augmentation for improving vehicle path prediction with recurrent neural networks.” *Sensors* 20, no. 15 (2020): 4279.
18. Bowles, M. *Machine Learning with Spark and Python: Essential Techniques for Predictive Analytics.* John Wiley & Sons, 2019.
19. Jiang, C., H. Zhang, Y. Yue, and X. Hu. ”AM-YOLO: Improved YOLOV4 based on attention mechanism and multi-feature fusion.” In *2022 IEEE 6th Information Technology and Mechatronics Engineering Conference (ITOEC)*, vol. 6, 1403–1407. IEEE. (March 2022).
20. Li, K., F. Zhang, and J. Xiao. ”Maximum Entropy based Local Multiple Patterns for Texture Classification.” In *2021 IEEE 6th International Conference on Signal and Image Processing (ICSIP)*, 345–349. IEEE. (October 2021).
21. https://github.com/raimundo2019/revista.git